


**CASE REPORT**

# Aventriculi associated with holoprosencephaly in a dog

Laura Barnard<sup>1</sup> | Alexane Durand<sup>2</sup> | Lauren Blume<sup>3</sup> | Laura Lee<sup>4</sup> |  
Starr Cameron<sup>5</sup> 

<sup>1</sup>Canada West Veterinary Specialists,  
Vancouver, British Columbia, Canada

<sup>2</sup>Department of Clinical Veterinary Sciences,  
University of Bern, Bern, Switzerland

<sup>3</sup>Veterinary Imaging Solutions LLC,  
Milton, Vermont

<sup>4</sup>Department of Pathological Sciences,  
University of Madison – Wisconsin, Madison,  
Wisconsin

<sup>5</sup>Department of Medical Sciences, University  
of Wisconsin – Madison, Madison, Wisconsin

**Correspondence**

Starr Cameron, Department of Medical  
Sciences, University of Wisconsin – Madison,  
2015 Linden Drive, Madison, WI 53706.  
Email: starr.cameron@wisc.edu

**Abstract**

**Case Description:** A 10-month-old neutered male mixed breed dog was presented for assessment of poorly controlled seizures.

**Clinical Findings:** Magnetic resonance imaging of the brain disclosed complete absence of the lateral and third ventricles and mesencephalic aqueduct. Postmortem computed tomographic (CT) imaging and positive contrast cisterno-ventriculography confirmed the lack of a contiguous ventricular system. However, histopathology identified the presence of vestigial lateral and third ventricles with hypoplastic choroid plexus, atresia of the third ventricle, and fused thalami, consistent with a diagnosis of lobar holoprosencephaly (HPE).

**Clinical Relevance:** To our knowledge, this report is the first case of radiographically confirmed aventriculi associated with HPE, a rare congenital malformation previously reported in people, to be described in veterinary medicine.

**KEYWORDS**

congenital, malformation, neuropathology, ventricles, ventriculogram

## 1 | SIGNALMENT, HISTORY, AND CLINICAL FINDINGS

A 10-month-old neutered male mixed breed dog weighing 26.4 kg was presented to the University of Wisconsin School of Veterinary Medicine for assessment of poorly controlled seizures. The dog previously had been found as a stray in a field at approximately 3 months of age with presumed littermates. Shortly after being rescued, the dog was noted to develop seizure activity, which initially was characterized as episodes of “staring off into space” and “fine tremoring.” These episodes progressed over several months to include generalized, tonic-clonic seizures with loss of consciousness, paddling movements of all 4 limbs, urination, and hypersalivation. The episodes often would occur in clusters (2–3 per 24-hour period) and include periods of status epilepticus (1 seizure was

described as lasting 18 minutes). Baseline laboratory testing (CBC and serum biochemistry) performed by the primary veterinarian 5 months before presentation (September 2017) showed no clinically relevant abnormalities. Phenobarbital was started at a total dose of 7.5 mg (0.5 mg/kg) PO q12h to obtain seizure control. Over the next several months, seizures continued to progress, and the dose was increased to 30 mg PO q12h as the dog grew in size. In December 2017, cluster seizures occurred; the dose of phenobarbital was increased to 60 mg PO q12h (2.3 mg/kg) and levetiracetam standard release (Keppra SR) was initiated at a dose of 500 mg PO q8h (20 mg/kg). Serum levetiracetam concentration was assessed in January 2018 and found to be 14.5 µg/mL (reference range, 5–45 µg/mL). Despite having a good temperament, the dog was noted to have poor house training and was unable to learn basic commands. The dog was suspected to be deaf with possible blindness in the left eye.

At the time of presentation to the University of Wisconsin, School of Veterinary Medicine in February 2018, general physical

**Abbreviations:** CSF, cerebrospinal fluid; CT, computed tomography; HPE, holoprosencephaly; MRI, magnetic resonance imaging.

This is an open access article under the terms of the Creative Commons Attribution-NonCommercial License, which permits use, distribution and reproduction in any medium, provided the original work is properly cited and is not used for commercial purposes.

© 2020 The Authors. *Journal of Veterinary Internal Medicine* published by Wiley Periodicals LLC. on behalf of the American College of Veterinary Internal Medicine.

examination was unremarkable. Initial neurological examination was performed shortly after a cluster of at least 4 seizures within the previous 48 hours. Mentation was mildly obtunded. Cranial nerve examination disclosed absent menace response in the left eye but was otherwise normal. The patient was nonambulatory but could walk with assistance. When supported, the dog was tetraparetic, worse on the left side, with generalized, moderate proprioceptive ataxia. Absent paw replacement was noted in the left thoracic limb and both pelvic limbs, and delayed paw replacement was noted in the right thoracic limb. Spinal reflexes were within normal limits and the patient was comfortable on spinal palpation. Current medications included phenobarbital 64.8 mg PO q12h and levetiracetam standard release 1000 mg PO q8h. Serum phenobarbital concentration measured the day before presentation was 21 µg/mL (reference range, 17–48 µg/mL).

Given the history and examination findings, neurolocalization was made to the thalamocortex with a possible predominance to the right side, considering the left-sided deficits. Differential diagnoses included congenital malformations, metabolic or degenerative disorders (eg, lysosomal storage disorder), inflammatory causes (infections such as protozoal, viral, fungal, bacterial, or immune-mediated), or neoplasia (primitive neuroectodermal tumor or other). Considering the lateralizing deficits present on neurologic examination, juvenile epilepsy was considered less likely.

## 2 | IMAGING AND PATHOLOGICAL FINDINGS

Thoracic radiographs were performed before magnetic resonance imaging (MRI) and were unremarkable. Magnetic resonance imaging of the brain was performed using a 1.5 Tesla magnet (GE Healthcare, 1.5 Tesla, Milwaukee, Wisconsin). Dorsal, sagittal and transverse T2-weighted (T2w) fast spin echo (FSE), transverse fluid attenuation inversion recovery (FLAIR), T2\*-weighted (T2\*w) gradient echo (GRE), and T1-weighted (T1w) pre- and postcontrast administration sequences were acquired. A 3-dimensional T1w spoiled gradient recalled echo (SPGR) postcontrast sequence also was performed.

All acquired sequences indicated absence of visible lateral ventricles, third ventricle, interventricular foramina, and mesencephalic aqueduct, and cerebrospinal fluid (CSF) volume was markedly decreased in the fourth ventricle (Figures 1 and 2). In T1-weighted postcontrast images, an enhancing choroid plexus was identified in the fourth ventricle, extending into the lateral apertures bilaterally. Faint linear enhancement also was present bilaterally in the region of the expected choroid plexuses of the lateral ventricles. Normal CSF signal was identified in the subarachnoid space of the quadrigeminal cistern, forming a characteristic “H-shape” in the dorsal T2w sequence<sup>1</sup> (Figure 3). Midline fusion of the bilateral thalamic components was noted, with absent visualization of a normal interthalamic adhesion on sagittal images. Similarly, the diencephalon and mesencephalon could not be clearly delineated because of the absent third ventricle and mesencephalic aqueduct. The corpus callosum was thin, and best appreciated at the level of the body (Figures 1 and 2). The longitudinal cerebral interhemispheric fissure, however, was intact. These findings were suggestive of atypical holoprosencephaly (HPE) with concurrent ventricular system atresia (aventriculi). Considering the results of the MRI and

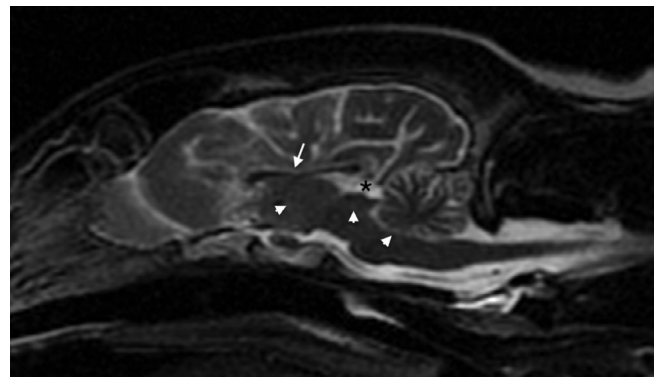
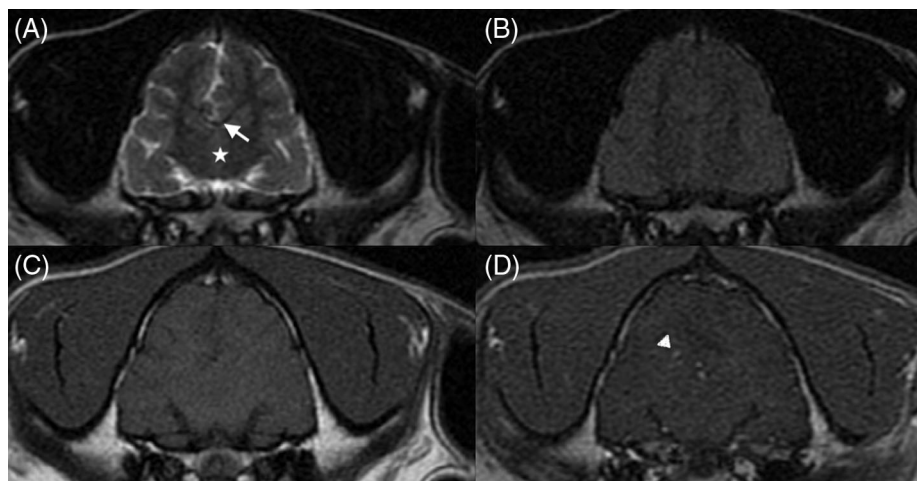


**FIGURE 1** Midsagittal T2w image of the brain, showing the absent third ventricle, absent mesencephalic aqueduct, and reduced CSF signal within the fourth ventricle (arrowheads). There is also thinning of the corpus callosum (arrow). The quadrigeminal cistern is normal (asterisk). CSF, cerebrospinal fluid

**FIGURE 2** A, Transverse T2w, B, FLAIR, C, Precontrast, and, D, Postcontrast T1w images of the brain at the level of the thalamus. Note the absence of visible lateral and third ventricles with fusion of the thalami (asterisk), as well as thinning of the corpus callosum (arrow). There was faint enhancement in the region of the expected choroid plexus of the right-sided lateral ventricle (D, arrowhead). FLAIR, fluid attenuation inversion recovery



concern for ongoing poor seizure control with no surgical options to correct the condition, the rescue group elected humane euthanasia.

After euthanasia, precontrast computed tomography (CT) of the dog's head was performed with the animal in sternal recumbency. The dog then was placed in right lateral recumbency and a cisternal CSF puncture performed using a 1.5-inch 22G spinal needle, yielding 2 mL of CSF. Leaving the spinal needle in place, a 3 mL syringe was attached and approximately 0.75 mL of positive contrast medium (Omnipaque [iohexol], 240 mg/mL solution) was instilled into the subarachnoid space until resistance was met. The caudal end of the dog was lifted so that its head was dependent, facilitating flow of contrast material cranially. A postcontrast CT scan (GE Healthcare LightSpeed

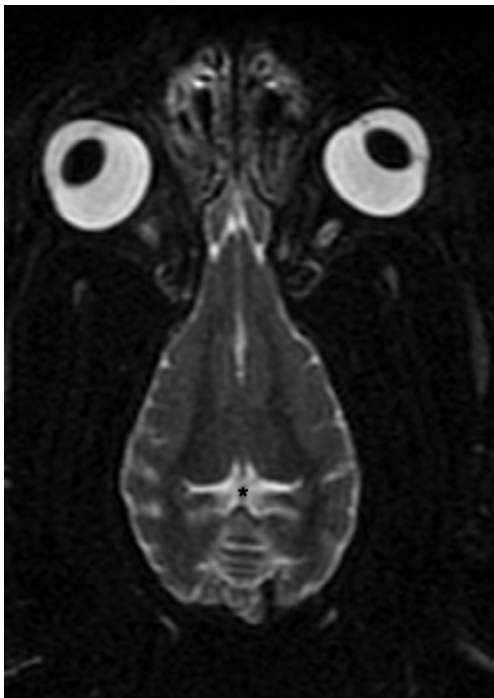


**FIGURE 3** Dorsal T2w image at the level of the quadrigeminal cistern, showing normal shape and filling

Ultra, Third Generation, 8 slice helical CT, Milwaukee, Wisconsin) then was performed with the dog in right lateral recumbency to assess for adequate rostral flow of the contrast medium, and immediately repeated with the dog in sternal recumbency. Images were obtained with a slice thickness of 0.625 mm, using both soft tissue and bone reconstruction algorithms. The positive contrast cisternovenriculography confirmed a lack of connection between the subarachnoid space of the cisternal puncture site and the ventricular system rostral to the fourth ventricle (Figure 4).

On gross examination, no distinct craniofacial defects were present. The interhemispheric fissure was irregular but extended to the level of the corpus callosum. The lateral ventricles were collapsed, and the third ventricle and mesencephalic aqueduct were collapsed and inapparent. Throughout the entire diencephalon, fusion of structures was present across midline, and rostrally, the diencephalon was displaced medial to the lateral ventricles and fused to the corpus callosum. Histopathologic examination identified vestigial lateral ventricles with irregular ependymal lining and hypoplastic choroid plexus (Figure 5). The third ventricle was vestigial dorsally, but most of the third ventricle was atretic and exhibited forking characterized by irregularly arranged rudimentary ependymal-lined canals in place of the normal ventricle (Figure 6). Similarly, the mesencephalic aqueduct was collapsed and slit-like with areas of atresia and forking. The fourth ventricle showed similar features, but in the lateral recess of the fourth ventricle, the associated choroid plexus was progressively elaborate, partially mineralized, and showed no evidence of hypoplasia. Multiple nuclei were abnormal and suspected to be poorly developed or dysplastic, including the putamen, globus pallidus, and the olivary nuclei, but without age- and breed-matched controls these changes could not be confirmed. Based on these histopathological findings, a diagnosis of lobar HPE was made.

### 3 | DISCUSSION

Holoprosencephaly is defined as a primary disorder of neural induction and patterning of the rostral neural tube, resulting in a primary

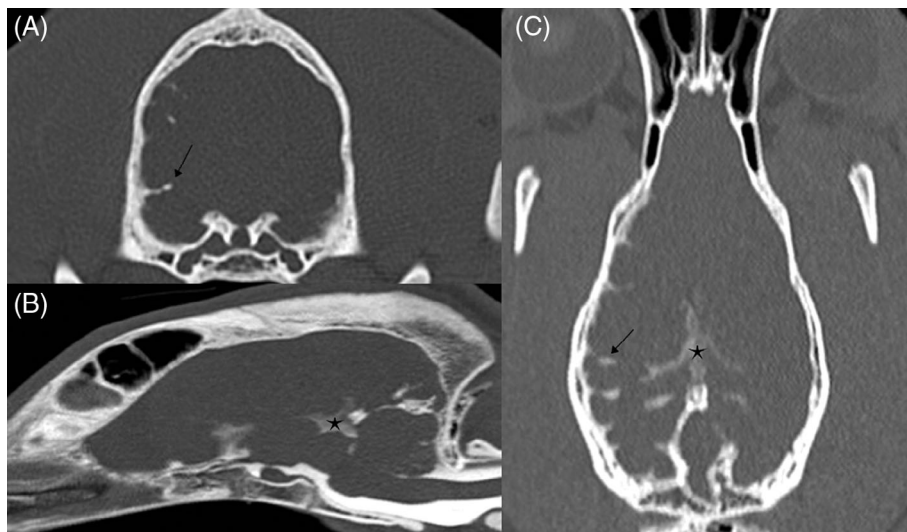


**FIGURE 4** A, Transverse, B, Sagittal, and, C, Dorsal CT images after immediate postmortem positive contrast cisternovenriculography. A, C, Note the lack of enhancement of the lateral ventricle, third ventricle, and mesencephalic aqueduct. The quadrigeminal cistern (asterisk) is normal. The sulci on the right side of the patient are more filled than the left, due to right lateral recumbency during cisternal injection. CT, computed tomography



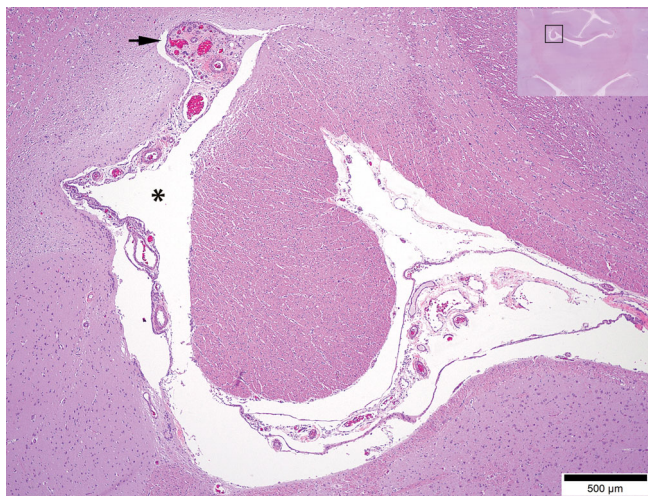


**FIGURE 5** Photomicrographs through the level of the diencephalon (inset) demonstrate a vestigial lateral ventricle (asterisk) and hypoplastic choroid plexus (arrow). H&E stain; Scale bar = 500  $\mu$ m

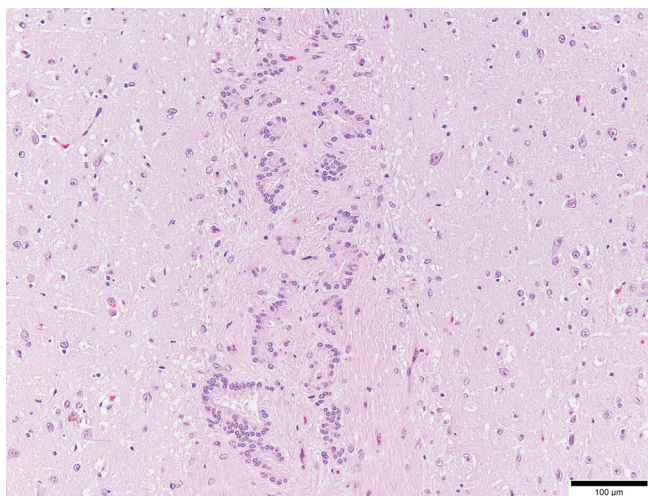


**FIGURE 6** Photomicrographs show that the third ventricle is composed of irregularly arranged rudimentary ependymal-lined canals, also known as "forking." H&E stain; Scale bar = 100  $\mu$ m

midline defect causing failed separation of forebrain (prosencephalon) structures.<sup>2</sup> It previously has been described in the veterinary literature in a Schnauzer dog, Morgan horse, cat, and in a case series examining corpus callosal abnormalities in dogs in which most cases also displayed HPE.<sup>3-6</sup> Holoprosencephaly presents with a wide spectrum of phenotypic variability and is grouped into several subtypes dependent on the extent of noncleavage present within the forebrain. These subtypes, in descending order of severity, include alobar, semi-lobar, lobar, and middle interhemispheric.<sup>2,7,8</sup> A newer subtype of HPE, termed *aventriculi*, is characterized by failed development of the ventricular system and has been described in the human medical literature since 1996.<sup>9</sup> To date, the human medical literature now includes several reports of this condition, including 4 cases of living patients and 1 of a premature infant that died 1 hour after birth.<sup>9-13</sup> Our report is the

first case of radiographically confirmed *aventriculi* and HPE in veterinary medicine.

Our dog shared several similarities with the clinical signs reported in the children in the human medical literature, including cortical blindness, deafness, seizures, and delayed development. In 1 case, a brainstem auditory evoked response (BAER) test was performed, which showed an absent waveform V, corresponding approximately with the termination of the lateral lemniscus within the inferior colliculus on the contralateral side.<sup>14</sup> Unfortunately, BAER testing was not performed to confirm the presence of hearing loss in our dog. Prior veterinary cases of HPE without *aventriculi* have described electrolyte disturbances and *adipsia* or *hypodipsia*, suspected to be secondary to abnormal formation of the hypothalamus.<sup>3</sup> Unfortunately, serum electrolyte concentrations were not determined in our dog, but *adipsia* or *hypodipsia* was not a component of the dog's history, and previous serum biochemistry and CBC results were normal.

Some differences were noted in the imaging characteristics between the cases in the human medical literature and our dog. All 4 human cases with *aventriculi* had absence of lateral and third ventricles, as well as lack of corpus callosum.<sup>9-12</sup> Variations included an absent fourth ventricle and fused thalami, inferior vermal hypoplasia and dilatation of the fourth ventricle (consistent with a Dandy Walker variant), severely dysplastic cerebral hemispheres, *polymicrogyria* or *pachygyria*, and *rhombencephalosynapsis*. Although an age- and breed-matched control was not available for direct comparison, our dog had thinning of the corpus callosum on MRI, which was consistent with the human cases of *aventriculi* and the classical veterinary forms of HPE. Additionally, nuclei including the putamen, globus pallidus, and olivary nuclei also appeared abnormal and poorly developed on histopathological evaluation. Interestingly, this male dog's malformations resembled characteristics described in the 2 male human patients, without any clear evidence of malformations within the caudal (posterior) fossa.

The underlying etiology of *aventriculi* is not clear in the human medical literature. One case description mentions a high rate of previous miscarriages in the mother. Another case had parents who were distantly related.<sup>11,12</sup> In total, 3 females and 2 males were reported with *aventriculi*, which does not support an X-linked trait. More classic cases of HPE in humans most commonly have been associated with a genetic syndrome, the most common being trisomy 13.<sup>15,16</sup> Other suggested possible causes of HPE include maternal diabetes, exposure to ethyl alcohol, cigarette smoking, and retinoic acid during pregnancy.<sup>16</sup> Similarly, sheep that ingest the steroid alkaloid *Veratrum californicum* early in gestation bear offspring with HPE, but it is accompanied by cyclopean malformation, which was neither present in our dog nor in living human patients with *aventriculi*.<sup>17</sup> No specific mutations or environmental exposures have been identified in humans that result in the *aventriculi* subtype of HPE. Because the remaining puppies in the litter were not showing signs of seizures or delays in training, it is speculated that a random genetic mutation, and not infection or toxin exposure, was most likely the cause of the *aventriculi*.

Histopathology of *aventriculi* associated with HPE in humans is limited to 1 case. Although our dog had a variably atretic ventricular system, the presence of a hypoplastic choroid plexus and irregular

ependymal lining was most consistent with the histopathologic diagnosis of lobar HPE, vestigial lateral and third ventricle, and third ventricle atresia. Many cases of HPE result in a monoventricle, which subsequently may lead to hydrocephalus, which is suspected to occur secondary to third ventricular obstruction resulting from inappropriate division of the thalami. Alternatively, in less severely affected cases (ie, lobar HPE) no overt ventricular abnormalities may be present. Because the choroid plexus is responsible for secretion of CSF, absence of a well-developed choroid plexus in this dog could have prevented development of hydrocephalus and an enlarged monoventricle. Choroid plexus hypoplasia has been associated with a defect in sonic hedgehog gene signaling.<sup>18</sup> Interestingly, our dog had a complete interhemispheric fissure with a monoventricle that was formed ventral to an intact corpus callosum as opposed to ventral to fused hemispheres, a feature not typical of any of the HPE variants.

Aventriculi, as a component of HPE, has not been described previously in the veterinary literature. This congenital malformation should be considered as a possible differential diagnosis in a young animal that is experiencing intractable seizure activity. Findings on MRI, or CT with positive contrast ventriculography, are diagnostic for this condition. Long-term prognosis of this condition in dogs remains unknown because of the euthanasia of this patient at the time of diagnosis.

#### CONFLICT OF INTEREST DECLARATION

Authors declare no conflict of interest.

#### OFF-LABEL ANTIMICROBIAL DECLARATION

Authors declare no off-label use of antimicrobials.

#### INSTITUTIONAL ANIMAL CARE AND USE COMMITTEE (IACUC) OR OTHER APPROVAL DECLARATION

Authors declare no IACUC or other approval was needed.

#### HUMAN ETHICS APPROVAL DECLARATION

Authors declare human ethics approval was not needed for this study.

#### ORCID

Starr Cameron  <https://orcid.org/0000-0001-5009-2546>

#### REFERENCES

- Bertolini G, Ricciardi M, Caldin M. Multidetector computed tomographic and low-field magnetic resonance imaging anatomy of the quadrigeminal cistern and characterization of supracollicular fluid accumulations in dogs. *Vet Radiol Ultrasound*. 2016;57(3):259-268.
- Fallet-Bianco C. Neuropathology of holoprosencephaly. *Am J Med Genet C Semin Med Genet*. 2018;178(2):214-228.
- Gonçalves R, Volk H, Smith PM, et al. Corpus callosal abnormalities in dogs. *J Vet Intern Med*. 2014;28(4):1275-1279.
- Koch T, Loretto A, de Lahunta A, Kendall A, Russell D, Bienzle D. Semilobar holoprosencephaly in a Morgan Horse. *J Vet Intern Med*. 2005;19(3):367-372.
- Shimbo G, Tagawa M, Yanagawa M, Miyahara K. MRI of lobar holoprosencephaly in a cat with hypodipsic hypernatraemia. *J Feline Med Surg Open Rep*. 2018;4(2):205511691880160.
- Shimokawa Miyama T, Iwamoto E, Umeki S, Nakaichi M, Okuda M, Mizuno T. Magnetic resonance imaging and clinical findings in a miniature schnauzer with hypodipsic hypernatremia. *J Vet Med Sci*. 2009;71(10):1387-1391.
- Monuki ES. The morphogen signaling network in forebrain development and holoprosencephaly. *J Neuropathol Exp Neurol*. 2007;66(7):566-575.
- Simon EM, Hevner RF, Pinter JD, et al. The middle interhemispheric variant of holoprosencephaly. *AJNR Am J Neuroradiol*. 2002;23(1):151-156.
- Garfinkle WB. Aventriculy: a new entity? *AJNR Am J Neuroradiol*. 1996;17(9):1649-1650.
- Sener RN. Aventriculi associated with holoprosencephaly. *Comput Med Imaging Graph*. 1998;22(4):345-347.
- Kumar S, Jaiswal AK, Rastogi M. Aventriculi associated with holoprosencephaly. *J Clin Neurosci*. 2006;13(3):378-380.
- Ciftcioglu E, Ozyurek H, Nural MS, Kopuz C, Incesu L, Ogur G. Absence of the lateral and third ventricles associated with holoprosencephaly. *Anat Cell Biol*. 2015;48(3):222-224.
- Laure-Kamionowska M, Szymanska K, Klepacka T. Holoprosencephaly with agenesis of the prosencephalic ventricle. *Folia Neuro-pathol*. 2015;4:387-394.
- Moller A. *Hearing: Anatomy, Physiology, and Disorders of the Auditory System*. 2nd ed. Cambridge, Massachusetts: Academic Press; 2006.
- Kruszka P, Muenke M. Syndromes associated with holoprosencephaly. *Am J Med Genet C Semin Med Genet*. 2018;178(2):229-237.
- Winter TC, Kennedy AM, Woodward PJ. Holoprosencephaly: a survey of the entity, with embryology and fetal imaging. *Radiographics*. 2015;35(1):275-290.
- Binns W, James LF, Shupe JL. Toxicosis of *Veratrum californicum* in ewes and its relationship to a congenital deformity in lambs. *Ann N Y Acad Sci*. 1964;111:571-576.
- Yang P. Central Role for Sonic Hedgehog-Triggered Pericytes in Hind-brain Choroid Plexus Development [PhD dissertation]. Harvard University; 2013.

**How to cite this article:** Barnard L, Durand A, Blume L, Lee L, Cameron S. Aventriculi associated with holoprosencephaly in a dog. *J Vet Intern Med*. 2020;34:2682-2686. <https://doi.org/10.1111/jvim.15907>